ACS OMEGA

Open Access

http://pubs.acs.org/journal/acsodf

Article

Simulation Study on Molecular Behavior of Rhamnolipids and Biobased Zwitterionic Surfactants at the Oil/Water Interface: Effect of Rhamnose Moiety Structures

Yamiao Zhang, Jianlong Xiu,* Lina Yi, Guangzhi Liao, Li Yu, and Lixin Huang

Cite This: *ACS Omega* 2023, 8, 36655−36661

Read Online

ACCESS | Metrics & More | Article Recommendations | Supporting Information

ABSTRACT: Molecular behavior of rhamnolipid mixed with a biobased zwitterionic surfactant at *an n*-hexadecane/water interface has been studied, and the effects of a rhamnose moiety and composition are evaluated. Results showed that rhamnolipid abundantly interacts with biobased surfactant EAB by means of hydrophobic interactions between aliphatic tails and electrostatic interactions between headgroups, including the attractive interaction between COO^- of rhamnolipids and N^+ of biobased surfactants and the repulsive interaction between COO^- of both surfactants. Dirhamnolipid has a larger number of bound Na^+ and a more stable bound structure of $COO^- \sim Na^+$, which screens the repulsive interaction between two kinds of surfactants and shows a more homogeneous distribution with biobased surfactants. The interfacial tension between *n*-hexadecane and water has been synergistically reduced by dirhamnolipids mixed with biobased surfactants at a higher molar ratio of biobased surfactants. Monorhamnolipids show a strengthened interaction with N^+ of biobased surfactants and a more stable hydrogen bond with water relative to that of dirhamnolipids, and there is no synergistic effect in lowering the interfacial tension for the mixture of monorhamnolipids and biobased surfactants. The present work provides details of the molecular behavior of biosurfactant rhamnolipids mixed with biobased surfactants and obtains the key factor in affecting the interfacial properties of the binary system.

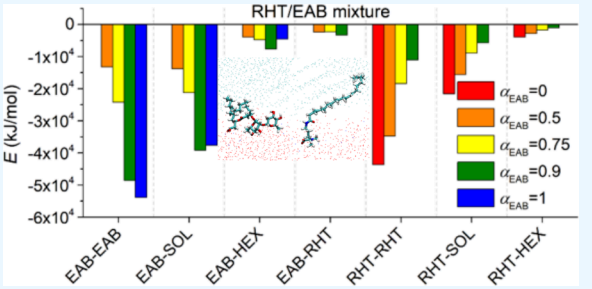

INTRODUCTION

Biosurfactants have attracted increasing attention due to their good interfacial activities in recent decades and become an alternative to synthetic surfactant. Rhamnolipids are one of the typical glycolipid biosurfactants and show structural diversities even from the same microbe and in the culture condition. It has been reported that rhamnolipids exhibit a synergistic effect in lowering liquid/liquid interfacial tension, micellization in solution, and adsorbing at the liquid/solid interface when mixing with synthetic surfactants and even other biosurfactants, which indicates a wide application of rhamnolipids combined with other surfactants in the industrial field that refer to the reduction of interfacial tension, emulsification, dispersion, and wetting alternation.[1]

Small-angle neutron scattering and neutron reflectivity results[2] showed that monorhamnolipids are mixed close-to-ideal with sodium dodecyl 6-benzenesulfonate (LAS) at the air−water interface, while LAS strongly partitions to the air−water interface relative to dirhamnolipids, probably due to the larger structure of dirhamnolipids. Synergistic adsorption of the rhamnolipid/LAS mixture, even the monorhamnolipid/dirhamnolipid/LAS ternary mixture, was found at the air/water interface.

When Euston[3] et al. studied the adsorption of rhamnolipids by means of molecular dynamics simulation, they found that there were differences in the adsorption and surface chemistry of rhamnolipid homologues. A single isolated rhamnolipid does not fully represent the adsorption behavior of molecules, because in reality, molecules are adsorbed in a tightly packed monolayer, and the behavior of a single surfactant is also affected by the interaction of other surfactants around in the molecular structure, two types of surfactants have two or more ionic properties of cation, anion or nonion at the same time.[4] The surfactant can be ionized in aqueous solution, which will reflect the properties of its anionic surfactant in one solution but may show the properties of cationic surfactants in another solution. Betaine[5] is a common amphoteric surfactant, which has good resistance to hard water, foaming, bactericidal, biodegradation and other characteristics, and good temperature and salt resistance.[6] It is one of the important surfactants for oil displacement in high-temperature salt reservoirs, which can effectively reduce the oil/water interfacial tension and greatly improve oil recovery in the tertiary recovery.

Received: April 4, 2023
Accepted: September 8, 2023
Published: September 29, 2023

https://doi.org/10.1021/acsomega.3c02253
ACS Omega 2023, 8, 36655−36661

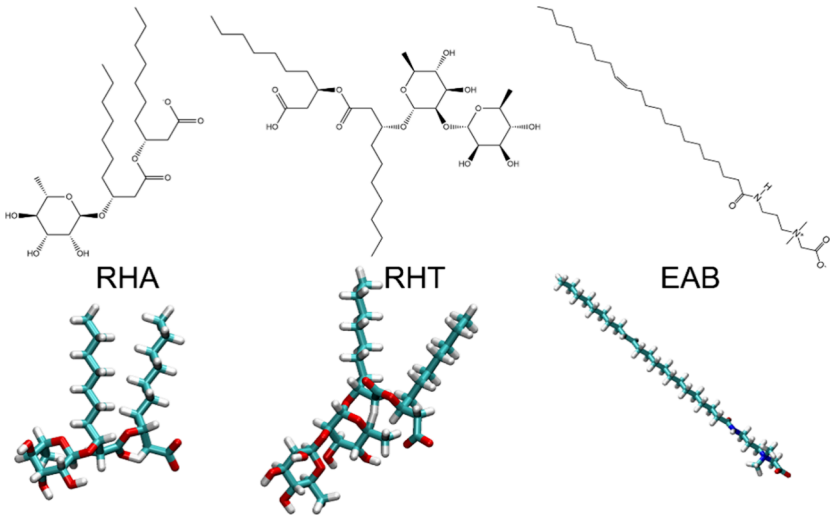

Figure 1. Chemical structures and topologies of rhamnolipids, $RhaC_{10}C_{10}$ (RHA) and $Rha_2C_{10}C_{10}$ (RHT), and biobased surfactants *N*-erucicamidopropyl-*N*,*N*-dimethyl carboxylbetaine (EAB). All the molecular structures are shown with VMD.[10]

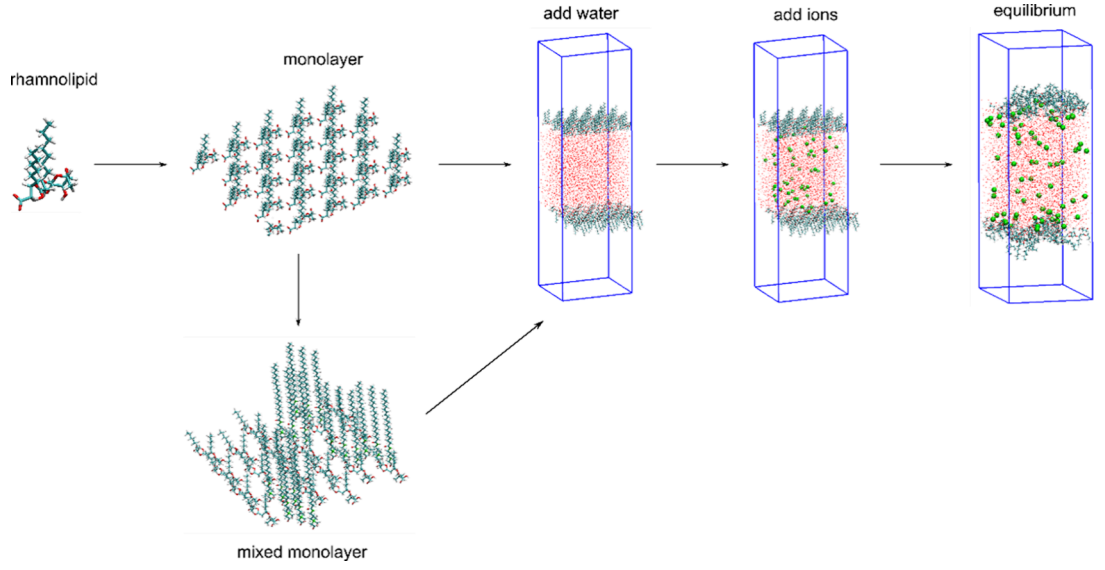

Figure 2. Strategy in simulating the individual surfactant monolayer and mixed surfactant monolayer at the *n*-hexadecane/aqueous solution interface.

Erucic amidopropyl betaine contains a long carbon chain in its molecular structure, which can effectively reduce the oil/water interfacial tension and form micellar gel of different strengths in salt solution or acid/alkali solution and can be used for acid thickening, clean fracturing fluid, and other aspects. Therefore, erucic amidopropyl betaine can be formulated into a variety of excellent oil and gas field working fluids, which has a huge demand in oil and gas field development.

In addition to lowering the air−water interface tension, rhamnolipids have been reported to primarily control the surface elasticity behavior when mixing with the commercially important zwitterionic surfactant cocamidopropyl betaine which leads to performance enhancements in terms of foam stability, and the rhamnolipid was proved to be the component in the mixture that tends to dominate at the air−water interface.[7] As for in solution, solubilization capabilities of rhamnolipids and synthetic nonionic surfactant Triton X-100 have been evaluated,[8] and the aqueous solubility of phenanthrene increased linearly with the total concentration of the rhamnolipid/Triton X-100 mixture, which would extend the rhamnolipid application. However, the difference in structure of rhamnolipid affecting the interfacial properties of binary system from the view of an atomistic level is still limited.

In the present study, two typical rhamnolipids, mono-rhamnolipid-C10C10 (RHA) and dirhamnolipid-C10C10 (RHT), are used to mix with the biobased surfactant, *N*-erucicamidopropyl-*N*,*N*-dimethyl carboxylbetaine (EAB), to form a mixed monolayer at the *n*-hexadecane/aqueous solution interface, and the interaction between the rhamnolipid and biobased surfactant has been investigated from the aspect of the structure of the monolayer, the spatial distribution of two kinds of surfactant, and the bound pairs formed between surfactants and between surfactants and solvation/cations. The present work aims to provide molecular details about how differences in the rhamnolipid structure affect the molecular behavior of the binary system.

https://doi.org/10.1021/acsomega.3c02253
ACS Omega 2023, 8, 36655−36661

Table 1. Number of Species and the Box Size in Molecular Dynamics Simulation

no.	RHA	RHT	EAB	Na^+	Cl^-	x (nm)	y (nm)
1	25 × 2	/	/	50	/	5.76112	4.77338
2	/	25 × 2	/	50	/	4.59405	7.50971
3	/	/	64 × 2	128	128	4.22078	5.45871
4	18 × 2	/	18 × 2	72	36	4.60890	5.70201
5	/	20 × 2	20 × 2	80	40	4.75328	7.32125
6	12 × 2	/	36 × 2	96	72	4.60890	5.67598
7	/	11 × 2	33 × 2	88	66	4.59405	5.89023
8	6 × 2	/	54 × 2	120	108	4.60890	5.64994
9	/	7 × 2	63 × 2	140	126	4.59405	7.03954

COMPUTATIONAL METHODS

The extended and all-trans conformation of the aliphatic tail was adopted to present the initial topology structure of RHA, RHT, and EAB surfactants (Figure 1). All of the individual simulation systems were constructed by the following steps (Figure 2). A box of simple point charge water[9] with a density of 0.9867 g/mL was generated first with a specific size in x and y directions (details in Table 1), and the water box was enlarged in the z axis to obtain two vacuum spaces. Then, two surfactant layers were arranged onto the two vacuum/water interfaces with their carboxyl groups dissolved in water. The molecular areas of RHA, RHT, and EAB were set as 1.10, 1.38, and 0.36 nm^2, respectively, according to experimental results. Na^+ and a certain amount of NaCl were introduced into the system by randomly replacing water, and the two vacuum spaces were further filled with n-hexadecane molecules with a density of 0.462 g/mL. As for the mixed system, two monolayers of RHA or RHT were first created, and certain amounts of RHA or RHT were randomly replaced by EAB molecules to obtain the mixed monolayer with a specific concentration of EAB (α_{EAB}).

Energy minimization was carried out using steepest descent method, and a 50 ns NPT simulation (323.2 K at 101.325 kPa) was performed after a short NVT simulation (298.2 K, 400 ps), which was followed by a short NPT simulation (298.2 K at 101.325 kPa, 200 ps). Detailed numbers of different species in each simulation system are shown in Table 1.

All the simulations were performed by Gromacs 4.6.7,[6] and OPLS-AA force fields[7] were employed, as formula, where r_{ij} is the distance between atom i and atom j, and ε_{ij} and σ_{ij} are the energy and size parameter. Temperatures were controlled by coupling to a thermostat using the v-rescale method[11,12] with a time constant of 0.1 ps. Berendensen and Parrinello−Rahman were used to maintain the semi-isotropic pressures of the systems in the 200 ps and the following 20 ns NPT simulations, respectively. The electrostatic interactions were calculated using the particle mesh Ewald method.[9] Cut-off radius for van der Waals and the real part of electrostatic interactions were 1.0 nm. All bonds were constrained with the LINCS algorithm. Thermodynamic equilibrium states were determined by monitoring the energies of the whole systems, and the last 20 ns trajectories, which have achieved equilibrium, with an interval time of data output of 1 ps were used for analysis. A 500 ps simulation was carried out for each system based on the final configuration of the 50 ns NPT simulation, and the trajectories were saved every 10 fs for the studies of dynamics of hydrogen bonds and the bound pairs between the surfactant and the cation.

$$U(r_{ij}) = 4\varepsilon_{ij}\left[\left(\frac{\sigma_{ij}}{r_{ij}}\right)^{12} - \left(\frac{\sigma_{ij}}{r_{ij}}\right)^{6}\right]$$

RESULTS AND DISCUSSION

Interfacial Properties of Surfactant Monolayers. Density distributions of the surfactant at the n-hexadecane/water interface (Figures 3a and S1) show that EAB has a much wider distribution along the normal to the interface in dependent on the composition of the mixed system, which can be attributed to the long and linear molecular structure. Headgroups of EAB go deep into water relative to that of rhamnolipid, and the aliphatic chain of EAB extended more into oil. Distributions of Na^+ focus at the interfacial region in the systems with lower α_{EAB}, and overlap with the distributions of COO^- from both EAB and rhamnolipid, which indicating the abundant interaction between Na^+ and COO^- of surfactants (Figures 3b and S2). Superiority distribution of Na^+ at interface vanish when the value of α_{EAB} increasing to 0.75, implying that abundant interaction between different species of surfactants occurred instead of interaction between surfactant and Na^+.

It can be observed that the distribution of the aliphatic tail of RHA covers the distribution of the headgroup, either in the individual RHA system or RHA/EAB binary systems. However, there is no complete overlap between distributions of the headgroup and aliphatic tail for RHT. These results suggest that the two rhamnose rings in RHT enhanced the hydrophilic property of the headgroup and orient deeply into water comparing with the two fatty acid chains. From the aspect of interfacial tension, synergistic effects happened in α_{EAB} = 0.5 RHA/EAB system, and the RHT/EAB system with α_{EAB} = 0.75 and 0.9. Interactions between surfactant molecules and between surfactants and cations/water are further studied to illustrate the synergistic effects in lowering the interfacial tension (Figure 4).

Interactions between Surfactant Molecules. It is clearly shown in Figure 5a that the location of the first peaks of the radial distribution functions of negative and positive moieties of EAB, COO^-, and N^+ around the COO^- group of RHA is nearly the same as those around RHT. It means that RHT distributed more homogeneously with EAB within the mixed monolayer, as shown in Figure 5b, although there is one more rhamnose ring in RHT comparing with the RHA molecule. It can be concluded that the COO^- group in rhamnolipids show close spatial distributions with both COO^- and N^+ in EAB, which suggests that there is abundant interaction between COO^- of rhamnolipid and COO^- of EAB, between COO^- of the rhamnolipid and N^+ of EAB. The

https://doi.org/10.1021/acsomega.3c02253
ACS Omega 2023, 8, 36655−36661

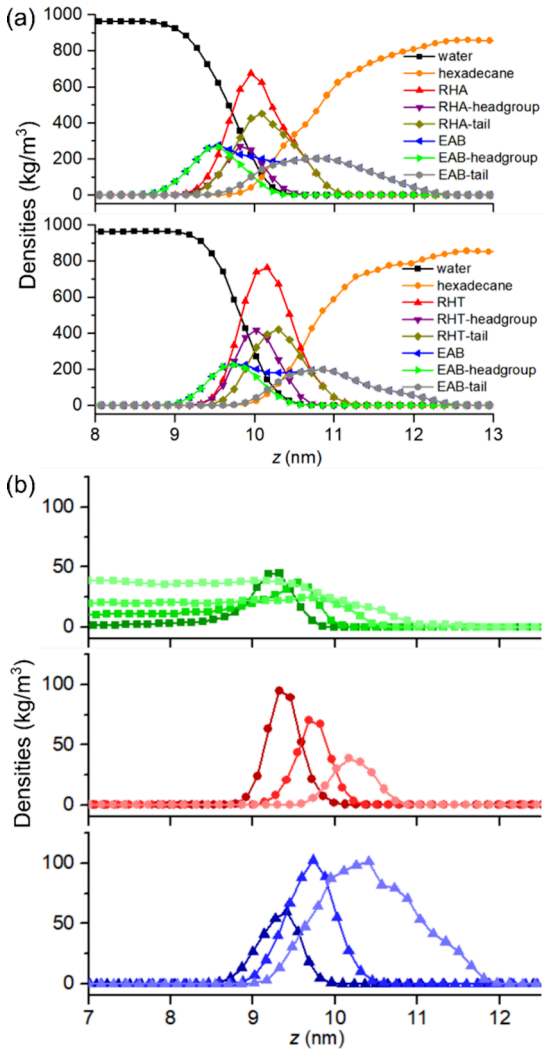

Figure 3. (a) Density distributions of water, *n*-hexadecane, surfactant, surfactant headgroup, and aliphatic tails in RHA/EAB and RHT/EAB systems, where α_{EAB} = 0.5; (b) density distributions of Na^+ (top, colors in dark to light denote that the values of α_{EAB} are 0, 0.5, 0.75, and 1, respectively), oxygens in the carboxyl group of RHA (middle, colors in dark to light denote that the values of α_{EAB} are 0, 0.5, and 0.75, respectively), and oxygens in the carboxyl group of EAB (bottom, colors in dark to light denote that the values of α_{EAB} are 0.5, 0.75, and 1, respectively) in RHA/EAB systems.

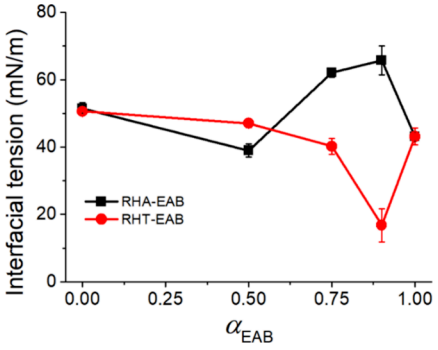

Figure 4. Interfacial tensions of *n*-hexadecane/aqueous solution along with the composition of the mixed monolayer.

former is definitely repulsive, and the latter is attractive. From the height of the peaks in radial distribution function curves,

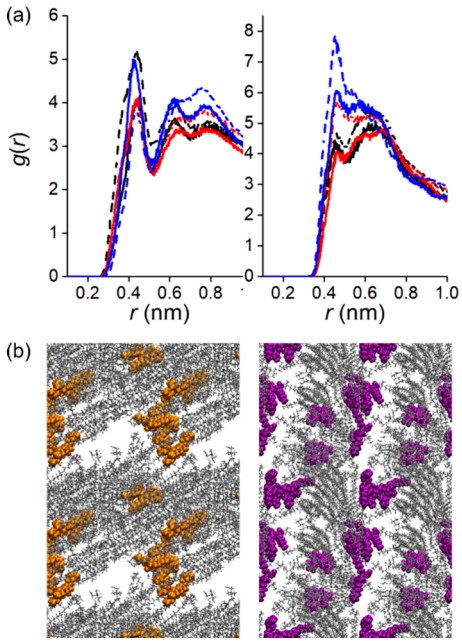

Figure 5. (a) Radial distribution function of oxygens (left) and nitrogen (right) in the carboxyl group of EAB with respect to the oxygens in the carboxyl group of RHA (dashed) or RHT (solid); black, red, and blue denote α_{EAB} = 0.5, 0.75, and 0.9, respectively. (b) Morphologies of the mixed monolayer of α_{EAB} = 0.5 RHA/EAB (left) and α_{EAB} = 0.5 RHT/EAB (right) systems. For clear display, RHA, RHT, and EAB molecules are shown in orange, purple, and gray, respectively.

the number of N^+ in EAB around the COO^- of RHA is more than those around the COO^- of RHT at the same α_{EAB}, which means that more attractive interactions exist between RHA and EAB. As for the number of COO^- in EAB around the COO^- of rhamnolipid, there is more COO^- of EAB around the COO^- of RHA than those of RHT when α_{EAB} = 0.5. As α_{EAB} = 0.75, the nearby number of COO^- is almost the same in both RHA/EAB and RHT/EAB systems. When α_{EAB} increases to 0.9, the number of COO^- in EAB around COO^- of RHT is obviously larger than those of RHA, which might be the factor leading to the lowest interfacial tension of α_{EAB} = 0.9 RHT/EAB system. Quan et al. found that when AuNPs were in low surface charge density, hydrophobic contact between the membrane core and the hydrophobic part of the ligand induced by lipid protrusion played a major role in the ability of AuNPs to penetrate the membrane core; when the AuNP has a high surface charge density, the attractive electrostatic interaction is dominant.[14]

In addition to the abundant electrostatic interaction between the headgroups of the surfactant, hydrophobic interactions between surfactant hydrophobic tails is another factor in affecting the intermolecular interaction within the mixed monolayer. Judging from the similar order parameter of hydrophobic tails, there are hydrophobic interactions between the rhamnolipid tail and EAB tail (Figures 6a and S3). The two aliphatic tails of RHA have nearly the same order parameter in individual RHA and mixed RHA/EAB systems, which means that the two tails have the same orientation, as shown in Figure 6b. Comparing with RHA, the two aliphatic tails of RHT have different order parameters, both values being smaller than those of RHA, which meant a more homogeneous orientation, as shown in Figure 6c.

https://doi.org/10.1021/acsomega.3c02253
ACS Omega 2023, 8, 36655−36661

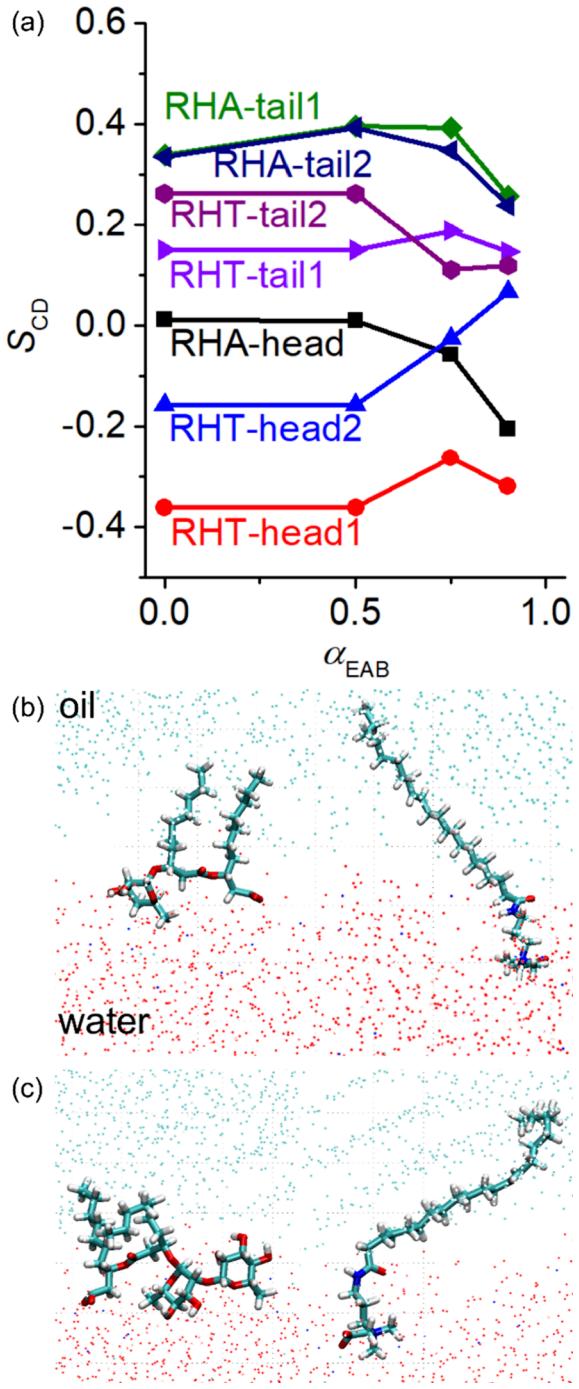

Figure 6. (a) Order parameters of vectors in the surfactant headgroup and aliphatic tail; (b) typical molecular orientation of RHA and EAB at the oil/water interface in α_{EAB} = 0.5 RHA/EAB system; (c) typical molecular orientation of RHT and EAB at the oil/water interface in α_{EAB} = 0.5 RHT/EAB system.

Order parameters of the two vectors in the RHT headgroup are close to −0.5, which means that the two rhamnose rings orient parallel to the interface. RHT has one more rhamnose ring than RHA, the larger headgroup anchoring at the oil/water interface, and has the orientation parallel to the interface. However, the huge structure of the headgroup makes RHT have a larger interfacial area, and the RHT aliphatic tails cannot fulfill the corresponding volume that is adjacent to oil. As a result, the RHT and EAB tails are disordered. Hess[13] obtained the critical micelle concentration (cmc), value of surface tension at cmc (γ_{cmc}), minimum area occupied by per surfactant molecule (A_{min}), and maximum adsorption capacity (Γ_{max}) RHA and RHT from their surface tension curves. The calculation results indicate that the A_{min} of RHA is slightly smaller than that of RHT, but the Γ_{max} of RHA is greater than that of RHT. Due to the small number of hydrophilic head groups, RHA is hydrophobic and easily adsorbed to the surface. In addition, due to the smaller molecular weight of RHA compared to RHT, the packing density of RHA molecules at the interface is higher than that of RHT molecules. The A_{min} of RHA is small, and its Γ_{max} is greater than RHT. With the increase of α_{EAB}, the orientation of EAB tails within the mixed RHT/EAB monolayer becomes more ordered and tilts at the interface. Especially in the α_{EAB} = 0.9 mixed RHT/EAB monolayer, EAB tails nearly perpendicular to the interface.

Interactions between the Surfactant and Na^+/Water. The number of water molecules that are hydrogen bonded to the carboxyl group of EAB, N_w, slightly reduces from 2.34 to 2.45 to 2.20, but N_w of RHA shows a 28.9% increase (Table 2). N_w of RHT shows values similar to those of N_w of RHA in the mixed system with the same α_{EAB}. Headgroups of EAB going deep into water make it have more hydrogen-bonded water molecules, and the wider exposure of the headgroup to water results in the resistance of N_w to composition change. As for the structure of hydrogen bonds formed between the carboxyl group and water, structural relaxation time of all the hydrogen bonds, τ, increases with the α_{EAB}, indicating that the structural stabilities of hydrogen bonds are strengthened. Structural stability of hydrogen bonds formed between RHA and water changes dramatically, and the value of τ is more than 2-fold longer when α_{EAB} increases from 0 to 0.9. It demonstrates that RHA interacts with solvent water more stable when mixing with EAB.

Numbers of Na^+ that are bound to carboxyl groups of surfactants to form ion pair decrease with increasing α_{EAB} (Table 3).[15,16] Numbers of bound Na^+ of EAB in RHA/EAB systems are similar to those in RHT/EAB systems. However, the reduction of bound Na^+ of RHT shows less reduction, 37.5%, relative to that of RHA, 60.4%. As shown in Figure 7a, the intermittent time correlation functions for the bound pairs between the carboxyl group of RHT and Na^+ relax more slowly than those formed between RHA and Na^+. More bound Na^+ and the more stable bound structure between Na^+ and RHT suggest the screen of the repulsive interaction between headgroups both from RHT or from RHT and EAB. These results are in accordance with the homogeneously distributed structure of the RHT/EAB monolayer obtained above.

Attractive interactions between rhamnolipid and EAB occur frequently with the increasing α_{EAB} because the bound pairs between the carboxyl group from rhamnolipids and N^+ of EAB increase, especially in the mixed RHA/EAB systems (Table 3). As shown in Figure 7b, the intermittent time correlation functions for the bound pairs between the carboxyl group of RHA and N^+ of EAB relax slowly than those formed between RHT and EAB.[17] More bound pairs and the more stable bound structure between COO^- and N^+ indicate the more abundant and strengthened attractive interaction between RHA and EAB when compared with those between RHT and EAB.

https://doi.org/10.1021/acsomega.3c02253
ACS Omega 2023, 8, 36655−36661

Table 2. Number of Water Hydrogen Bonded to Carboxyl Groups of RHA/RHT/EAB, N_w, and the Structural Relaxation Time of Hydrogen Bonds between Water and Surfactants, τ (ps)

		α_{EAB}				
		0	0.5	0.75	0.9	1
RHA/EAB system	N_w of RHA	1.14	1.30	1.40	1.47	
	N_w of EAB		2.34	2.36	2.26	2.20
RHT/EAB system	N_w of RHT	1.43	1.29	1.37	1.48	
	N_w of EAB		2.45	2.33	2.27	2.20
RHA/EAB system	τ of RHA-H_2O	31.63	44.71	72.68	105.51	
	τ of EAB-H_2O		39.80	42.98	69.38	89.58
RHT/EAB system	τ of RHT-H_2O	37.37	48.21	61.44	77.87	
	τ of EAB-H_2O		41.52	61.71	64.98	89.58

Table 3. Number of Na^+ Bound to Carboxyl Groups of EAB/RHA/RHT and the Bound Pairs of the Carboxyl Group of Rhamnolipids and N^+ of EAB

	RHA/EAB			RHT/EAB		
α_{EAB}	EAB-Na^+	RHA-Na^+	RHA-N^+	EAB-Na^+	RHT-Na^+	RHT-N^+
0		0.53			0.48	
0.5	0.30	0.47	1.55	0.17	0.47	1.16
0.75	0.24	0.30	2.97	0.22	0.45	2.42
0.9	0.18	0.21	4.40	0.19	0.30	3.91
1	0.14			0.14		

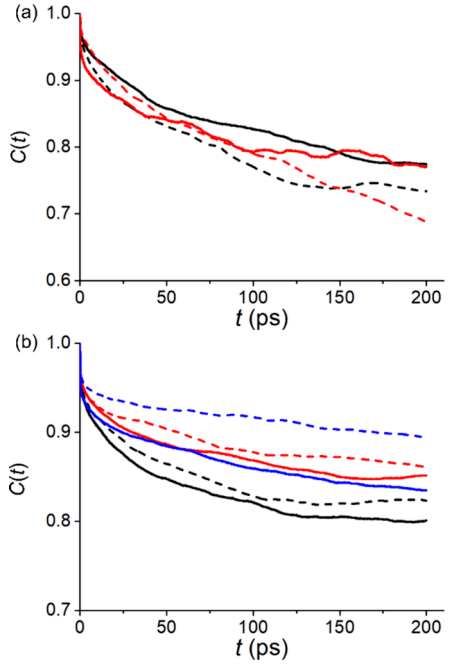

Figure 7. (a) Intermittent time correlation functions for the bound pairs between oxygen in the carboxyl group of RHA (dashed) /RHT (solid) and Na^+ in α_{EAB} = 0.5 (black) and α_{EAB} = 0.75 (red) mixed systems. (b) Intermittent time correlation functions for the bound pairs between oxygen in the carboxyl group of RHA (dashed) /RHT (solid) and N^+ in EAB of α_{EAB} = 0.5 (black), α_{EAB} = 0.75 (red), and α_{EAB} = 0.9 (blue) mixed systems.

CONCLUSIONS

Rhamnolipids as a kind of biosurfactants attract more attention due to their structural diversities, good interfacial properties, and renewable sources. The relationship between its structure and property becomes a key topic for researching and applying rhamnolipids. Molecular dynamics simulation has been employed to investigate the molecular behavior of typical rhamnolipids, $RhaC_{10}C_{10}$ and $Rha_2C_{10}C_{10}$, mixed with biobased surfactants at the *n*-hexadecane/water interface, which cannot be easily studied using the traditional experimental method.

Comparing with the structure of monorhamnolipids, dirhamnolipids have one more rhamnose ring, which enables the molecule to have a larger number of bound Na^+ and more stable bound structures of $COO^- \sim Na^+$, which screens the repulsive interaction between two kinds of surfactants and shows more homogeneous distribution with the biobased surfactant. Accordingly, the dirhamnolipids mixed with the biobased surfactant show a synergistic effect in lowering the interfacial tension between *n*-hexadecane and water at a higher molar ratio of the biobased surfactant. However, monorhamnolipids mixing with biobased surfactants have no synergistic effect in lowering the interfacial tension, although it shows strengthened interactions with N^+ of the biobased surfactant and a more stable hydrogen bond with water relative to that of dirhamnolipids. The results of this work provide insights into the effect of the rhamnolipid structure on the interfacial properties of the binary system of rhamnolipids and biobased surfactants.

ASSOCIATED CONTENT

Supporting Information

The Supporting Information is available free of charge at https://pubs.acs.org/doi/10.1021/acsomega.3c02253.

Density distribution of water, *n*-hexadecane, surfactant, surfactant headgroup, and aliphatic tail group in different systems; density distributions of Na^+, oxygens in the carboxyl group of RHT, and oxygens in the carboxyl group of EAB in RHT/EAB systems; order parameters of vectors in the EAB headgroup and aliphatic tail; and intermittent time correlation functions for the bound pairs between oxygen in different systems (PDF)

RHA and RHT data (ZIP)

AUTHOR INFORMATION

Corresponding Author

Jianlong Xiu − *PetroChina Research Institute of Petroleum Exploration and Development, Beijing 100083, People's Republic of China;* orcid.org/0009-0005-9004-0755; Email: xiujianlong@foxmail.com

Authors

Yamiao Zhang − *University of Chinese Academy of Sciences, Beijing 100190, People's Republic of China; Institute of Porous Flow and Fluid Mechanics, Chinese Academy of*

https://doi.org/10.1021/acsomega.3c02253
ACS Omega 2023, 8, 36655−36661

Sciences, Langfang 065007 Hebei Province, People's Republic of China; PetroChina Research Institute of Petroleum Exploration and Development, Beijing 100083, People's Republic of China

Lina Yi − *PetroChina Research Institute of Petroleum Exploration and Development, Beijing 100083, People's Republic of China*

Guangzhi Liao − *PetroChina Exploration and Production Company, Beijing 100120, People's Republic of China*

Li Yu − *PetroChina Research Institute of Petroleum Exploration and Development, Beijing 100083, People's Republic of China*

Lixin Huang − *PetroChina Research Institute of Petroleum Exploration and Development, Beijing 100083, People's Republic of China*

Complete contact information is available at: https://pubs.acs.org/10.1021/acsomega.3c02253

Notes

The authors declare no competing financial interest.

■ ACKNOWLEDGMENTS

This work was done with the financial support of the China National Petroleum Corporation (CNPC) Science and Technology Development Project (No. 2021DJ1605).

■ REFERENCES

(1) Chebbi, Alif; Franzetti, Andrea; Formicola, Francesca; Ambaye, Tekilt Gebregiorgs; Gomez, Franco Hernan; Murena, Beatrice; De Marco, Emanuela; Beltrani, Tiziana; Sbaffoni, Silvia; Vaccari, Mentore Insights into rhamnolipid-based soil remediation technologies by safe microorganisms: A critical review. *J. Cleaner Prod.* **2022**, *367*, 0959−6526.

(2) Euston, S. R.; Banat, I. M.; Salek, K. Congener-dependent conformations of isolated rhamnolipids at the vacuum-water interface: a molecular dynamics simulation. *J. Colloid Interface Sci.* **2021**, *585*, 148−157.

(3) Liu, Gaige; Li, Xiangkun; Zhang, Ruijun; Ma, Xiaochen; Xie, Hongwei Enhancing the decomposition and volatile fatty acids production of excess sludge: Synergistic pretreatment by endogenous lysozyme and rhamnolipid. *Fuel* **2022**, 323.

(4) Alargova, R. G.; Vakarelsky, I. Y.; Paunov, V. N.; Stoyanov, S. D.; Kralchevsky, P. A.; Mehreteab, A.; et al. Properties of amphoteric surfactants studied by zeta-potential measurements with latex particles. *Langmuir* **2003**, *14* (8), 1996−2003.

(5) Mouton, J.; Mercier, G.; Blais, J. F. Amphoteric surfactants for pah and lead polluted-soil treatment using flotation. *Water Air Soil Pollut.* **2009**, *197* (1−4), 381−393.

(6) Qing, Shao; Jiang, Shaoyi Influence of charged groups on the properties of zwitterionic moieties: a molecular simulation study. *J. Phys. Chem. B* **2014**, *118* (27), 7630−7637.

(7) Rekiel, Edyta; Zdziennicka, Anna; Szymczyk, Katarzyna; Jańczuk, Bronisław Thermodynamic Analysis of the Adsorption and Micellization Activity of the Mixtures of Rhamnolipid and Surfactin with Triton X-165. *Molecules* **2022**, *27*, 3600.

(8) Zhang, Yi; Placek, Tess L.; Jahan, Ruksana; Alexandridis, Paschalis; Tsianou, Marina Rhamnolipid Micellization and Adsorption Properties. *Int. J. Mol. Sci.* **2022**, *23* (19), 11090.

(9) Chen, M. L.; Penfold, J.; Thomas, R. K.; Smyth, T. J. P.; Perfumo, A.; Marchant, R.; Banat, I. M.; Stevenson, P.; Parry, A.; Tucker, I. Mixing Behavior of the Biosurfactant, Rhamnolipid, with a Conventional Anionic Surfactant. Sodium Dodecyl Benzene Sulfonate. *Langmuir* **2010**, *26* (23), 17958−17968.

(10) Yao, Zhou; Swara, Harne; Amin, Samiul Optimization of the surface activity of biosurfactant-surfactant mixtures. *J. Cosmet. Sci.* **2019**, *70* (3), 127−136.

(11) Zielkiewicz, J. Structural properties of water: comparison of the SPC, SPCE, TIP4P, and TIP5P models of water. *J. Chem. Phys.* **2005**, *123* (10), No. 104501.

(12) Humphrey, W. F.; Dalke, A.; Schulten, K. VMD: Visual molecular dynamics. *J. Mol. Graphics* **1996**, *14* (1), 33−38. 27−8

(13) Hess, B.; Kutzner, C.; Spoel, D. V. D.; Lindahl, E. GROMACS 4: Algorithms for highly efficient, load-balanced, and scalable molecular simulation. *J. Chem. Theory Comput.* **2008**, *3*, 435−447.

(14) Kaminski, George A.; Friesner, Richard A.; Tirado-Rives, Julian; Jorgensen, William L. Evaluation and Reparametrization of the OPLS-AA Force Field for Proteins via Comparison with Accurate Quantum Chemical Calculations on Peptides†. *J. Phys. Chem. B* **2001**, *105*, 6474−6487.

(15) Bussi, G.; Donadio, D.; Parrinello, M. Canonical sampling through velocity-rescaling. *J. Chem. Phys.* **2007**, *126*, No. 014101.

(16) Essmann, U.; Perera, L.; Berkowitz, M. L.; Darden, T.; Lee, H.; Pedersen, L. G. A smooth particle mesh ewald method. *J. Chem. Phys.* **1995**, *103* (19), 8577−8593.

(17) Quan, Xuebo; et al. Molecular Understanding of the Penetration of Functionalized Gold Nanoparticles into Asymmetric Membranes. *Langmuir ACS J. Surf. Colloids* **2016**, No. 6b02937.